Journal of Electroanalytical Chemistry 689 (2013) 216–222

Contents lists available at SciVerse ScienceDirect

Journal of Electroanalytical Chemistry

journal homepage: www.elsevier.com/locate/jelechem

Electrochemical oxidation mechanism of phosphotyrosine at a glassy carbon electrode

Oana M. Popa [a,b], Victor C. Diculescu [a,*]

[a] Departamento de Química, Faculdade de Ciências e Tecnologia, Universidade de Coimbra, 3004-535 Coimbra, Portugal
[b] Faculty of Physics, University of Bucharest, 077125 Magurele-Bucharest, Romania

ARTICLE INFO

Article history:
Received 31 May 2012
Received in revised form 10 October 2012
Accepted 5 November 2012
Available online 24 November 2012

Keywords:
Electrochemistry
Phosphotyrosine
Redox mechanism
Glassy carbon electrode

ABSTRACT

Protein phosphorylation by kinases plays a significant role in a wide range of cellular processes. Phosphotyrosine is the product of tyrosine phosphorylation. The electrochemical behaviour of phosphotyrosine (pTyr) at a glassy carbon electrode was investigated over a wide pH range, using cyclic, differential pulse and square-wave voltammetry. The oxidation is an irreversible, pH-independent process that involves the transfer of one electron and no proton. The oxidation of phosphotyrosine occurs in a cascade mechanism and for acid electrolytes one electroactive product was observed. In neutral and alkaline electrolytes two redox products that undergo reversible, pH-dependent redox reactions with the transfer of two electrons and two protons were characterised. Also, the oxidation of tyrosine was studied in order to find information about the redox products of phosphotyrosine. A redox mechanism for phosphotyrosine was proposed. The present study provides information concerning an electroanalytical signal for studying protein phosphorylation processes.

1. Introduction

Protein kinases represent a class of enzymes that modify other proteins through the chemical addition of a phosphate group from an ATP molecule to an aminoacid residue on a substrate protein, in a process named phosphorylation [1,2]. Protein phosphorylation is an important mechanism in transduction of extracellular signals to the cell interior and results in functional modifications of the target substrate protein by changing its activity, cellular location, or association with other biomolecules. Phosphorylation processes are responsible for the regulation of cell proliferation, differentiation and transformation [3,4]. Uncontrolled signalling is a frequent cause for inflammatory responses that leads to diseases such as cancer [5], atherosclerosis [6], and central nervous system disorders [7].

Kinases activity can be differentiated according to the phosphorylated aminoacid [8]. Although several phosphorylated residues such as thioesters of cysteine, phosphoramidates of lysine and histidine, and acid anhydrides of glutamic and aspartic acid have been identified, the most commune phophorylated residues in proteins are tyrosine, Scheme 1A, serine and threonine [9].

As most protein kinases, the tyrosine kinases play an important role in regulation of normal cell signalling pathway and, its high levels in tumor cell lines is a relevant biological aspect [10]. Most tyrosine-specific protein kinases are associated with the epidermal (EGF) [11] and platelet-derived (PDGF) [12] growth factors, and with the transforming proteins such as *v-src* and *v-abl* [13,14]. Identification of proteins containing phosphotyrosine, Scheme 1B, is important both, from the enzymological view point and from the elucidation of malignant transformation mechanisms.

Protein kinase activity is usually investigated by fluorescence, radioactive labelling, and Raman spectroscopy systems that involve enzymatic reactions or specific antibodies [15–19]. Simple methods for the systematic analyses of phosphorylation in a rapid and high-throughput manner are desired in order to enable kinase activity profiling for diagnostic applications and fast *in vitro* elucidation of cellular signal transduction pathways.

The use of the electrochemical methods were proved to be advantageous due to their fast response and sensitivity in detecting compounds at concentrations of ato- and femto-moles level, allowing direct measurement in biological samples with very little or no sample pre-treatment [20,21]. The electrochemical investigation in the field of protein phosphorylation has led to the development of biosensors for the detection of phosphorylation processes and small inhibiting molecules, which use post-labelling procedures [22] but a label-free electrochemical method for the detection of small-molecule inhibition of tyrosine phosphorylation was also described [23,24]. Nevertheless, these methods present disadvantages since there are many phenomena that can lead to the loss of electrochemical signals in complex samples (e.g. electrode fouling and/or non-specific adsorption).

* Corresponding author. Address: Instituto Pedro Nunes, Laboratório de Electroanálise e Corrosão, Rua Pedro Nunes, 3030-199 Coimbra, Portugal. Tel.: +351 239 700 943; fax: +351 239 700 912.
E-mail address: victorcd@ipn.pt (V.C. Diculescu).

1572-6657/$ - see front matter © 2012 Elsevier B.V. All rights reserved.
http://dx.doi.org/10.1016/j.jelechem.2012.11.005

Phosphotyrosine is electroactive [25] and its oxidation peak can represent an analytical signal useful for the development of new methodologies for studying protein phosphorylation processes. The electroactivity of phosphotyrosine has been studied in specific conditions such as pH 6.5 by cyclic and linear sweep voltammetry [25], but a systematic investigation of the redox mechanism of phosphotyrosine has not been yet undertaken.

The present study is concerned with the investigation of phosphotyrosine redox mechanisms at a glassy carbon electrode over a wide pH range, using cyclic (CV), differential pulse (DPV) and square-wave voltammetry (SWV).

2. Experimental

2.1. Materials and reagents

Phosphotyrosine (pTyr) and tyrosine (Tyr) were obtained from Sigma–Aldrich and used without purification. All supporting electrolyte solutions, Table 1, were prepared using analytical grade reagents and purified water from a Millipore Milli-Q system (conductivity $\leqslant 0.1\ \mu S\ cm^{-1}$). Stock solutions of 5 mM pTyr and 1 mM Tyr were prepared in deionized water and kept at −4 °C until further utilisation. Solutions of different concentrations of pTyr and Tyr were obtained by dilution of the appropriate volume in supporting electrolyte.

Nitrogen saturated solutions were obtained by bubbling high purity N_2 for a minimum of 10 min, and were maintained under superficial and constant N_2 flow during the voltammetric experiments.

Microvolumes were measured using EP-10 and EP-100 Plus Motorized Microlitre Pippettes (Rainin Instrument Co., Inc., Woburn, USA). The pH measurements were carried out with a Crison microph 2001 pH-metre with an Ingold combined glass electrode. All experiments were done at room temperature (25 ± 1 °C).

2.2. Voltammetric parameters and electrochemical cells

Voltammetric experiments were carried out using a Compact-Stat.e running with IviumSoft 1.918, Ivium Technologies, The Netherlands. The measurements were carried out using a three-electrode system in a 0.5 mL one-compartment electrochemical cell. A glassy carbon (GCE, d = 1.0 mm), a Pt wire, and a Ag/AgCl (3 M KCl) were used as working, auxiliary and reference electrodes, respectively.

The experimental conditions for differential pulse voltammetry were: pulse amplitude of 50 mV, pulse width of 100 ms and scan rate of 5 mV s^{-1}. For square wave voltammetry a frequency of 50 Hz and a potential increment of 2 mV, corresponding to an effective scan rate of 100 mV s^{-1} were used.

The GCE was polished using diamond spray, particle size 3 μm (Kemet, UK) before each electrochemical experiment. After polishing, it was rinsed thoroughly with Milli-Q water. Following this mechanical treatment, the GCE was placed in buffer supporting electrolyte and differential pulse voltammograms were recorded until a steady state baseline voltammogram was obtained. This procedure ensured very reproducible experimental results.

Table 1
Supporting electrolytes, 0.1 M ionic strength.

pH	Composition
2.3	HCl + KCl
3.4	HAcO + NaAcO
4.3	HAcO + NaAcO
5.1	HAcO + NaAcO
5.6	HAcO + NaAcO
6.0	$NaH_2PO_4 + Na_2HPO_4$
7.0	$NaH_2PO_4 + Na_2HPO_4$
8.0	$NaH_2PO_4 + Na_2HPO_4$
9.2	$NH_3 + NH_4Cl$

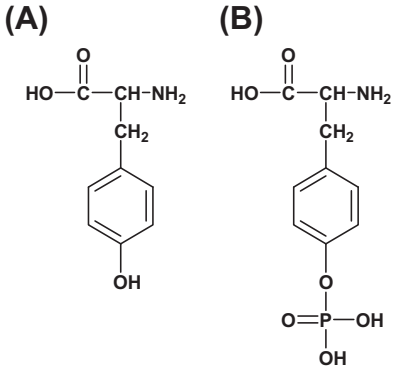

Scheme 1. Chemical structures of: (A) tyrosine and (B) phosphotyrosine.

2.3. Acquisition and presentation of voltammetric data

All differential pulse and square wave voltammograms presented were smoothed and baseline-corrected using an automatic function included in the IviumSoft version 1.918. This mathematical treatment improves the visualization and identification of peaks over the baseline without introducing any artefact, although the peak current is in some cases reduced (<10%) relative to that of the untreated curve. Nevertheless, this mathematical treatment of the original voltammograms was used in the presentation of all experimental voltammograms for a better and clearer identification

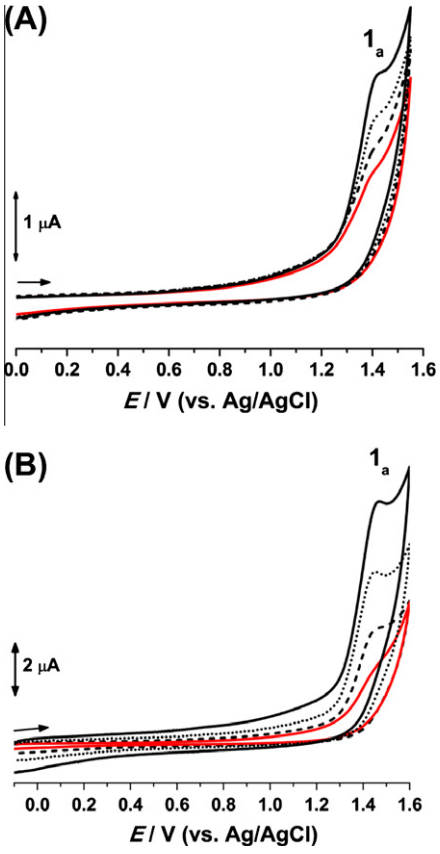

Fig. 1. Cyclic voltammograms in: (A) (—) 100, (- - -) 150, (···) 200 and (––) 250 μM phosphotyrosine in pH = 7.0 at v = 100 mV s^{-1} and (B) 500 μM phosphotyrosine in pH = 7.0 at (—) 25, (- - -) 100, (···) 250 and (––) 500 mV s^{-1}.

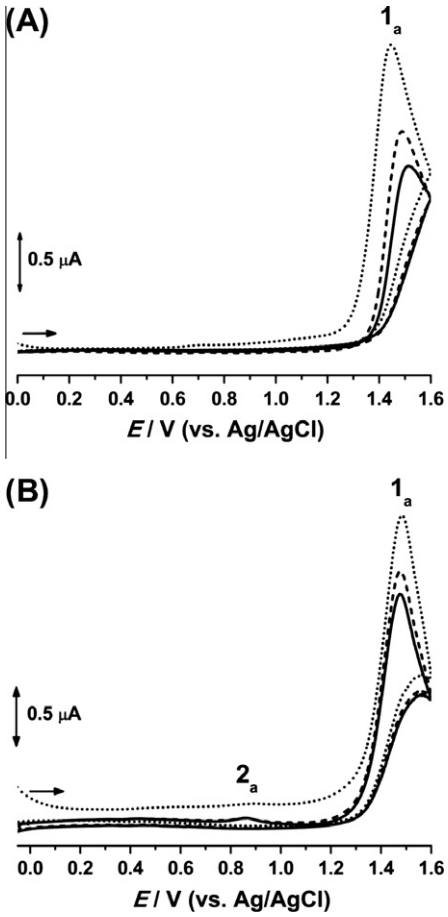

Fig. 2. Cyclic voltammograms base-line subtracted in 500 μM phosphotyrosine in: (A) pH = 7.0 and (B) pH = 3.4; (···) first, (- - -) second and (––) third scans at $v = 100$ mV s^{-1}.

of the peaks. The values for peak current presented in all graphs were determined from the original untreated voltammograms.

3. Results and discussion

3.1. Cyclic voltammetry

The electrochemical behaviour of phosphotyrosine (pTyr) was initially investigated by CV at $v = 100$ mV s^{-1} in solutions of 500 μM pTyr, in N_2 saturated electrolytes with different pH values. The CVs were recorded in the interval between −1.0 V and +1.5 V, starting from 0.0 V towards positive or negative potential limits. The results showed that pTyr undergoes only oxidation at the GCE and for this reason all subsequent experiments were carried out in the anodic region.

CV was performed in solutions of different concentrations of pTyr in pH = 7.0, Fig. 1A. Between voltammograms the GCE surface was always renewed in order to avoid possible interferences with the adsorption of pTyr and/or its oxidation products at the electrode surface. One main anodic peak 1_a was always observed and its current increased with solution concentration, Fig. 1A.

Cyclic voltammograms were obtained for different scan rates in a solution of 500 μM pTyr in pH = 7.0, Fig. 1B. Between measurements, the electrode surface was always polished in order to ensure a clean surface. The current of peak 1_a increased with increasing the scan rate.

Successive cyclic voltammograms were recorded in solution of 500 μM pTyr in electrolytes with different pH values.

At pH = 7.0, on the first anodic scan, peak 1_a occurred at $E_{p1a} = +1.43$ V, Figs. 2A and S1A. In the reverse scan no cathodic correspondent was observed, in agreement with the irreversibility of pTyr oxidation reaction. The peak 1_a current decreased in successive voltammograms and its potential turned more positive, Fig. 2A. These effects were due to the adsorption of pTyr and its oxidation products at the GCE surface, which reduced the available electrode surface area.

At pH = 3.4, the cyclic voltammograms recorded in solution pTyr have shown on the first anodic scan, peak 1_a at $E_{p1a} = +1.44$ V, Figs. 2B and S1B. By increasing the number of scans, a new irreversible peak 2_a occurred at $E_{p2a} = +0.86$ V. This peak was due to the oxidation of pTyr oxidation product formed at the GCE surface during the first scan.

3.2. Differential pulse voltammetry

3.2.1. Phosphotyrosine

The electrochemical oxidation of pTyr was studied over a wide pH range between 2.3 and 12.0 using DPV. The DP voltammograms were all recorded in a solution of 100 μM pTyr in different electrolytes with 0.1 M ionic strength, Fig. 3A. Peak 1_a occurred for $2.3 < pH < 9.0$. For higher pH values, no oxidation peak was obtained even for higher concentrations, showing that pTyr is not oxidisable in these conditions.

The potential of peak 1_a occurred at $E_{p1a} = +1.35$ V, independent on the pH of the supporting electrolyte, Fig. 3B. This is specific to an electrochemical reaction that involves only the transfer of electrons and no proton. In addition, the width at half height of peak 1_a was found to be $W_{1/2} \sim 90$ mV, close to the theoretical value correspondent to an electrochemical reaction involving the transfer of one electron [26].

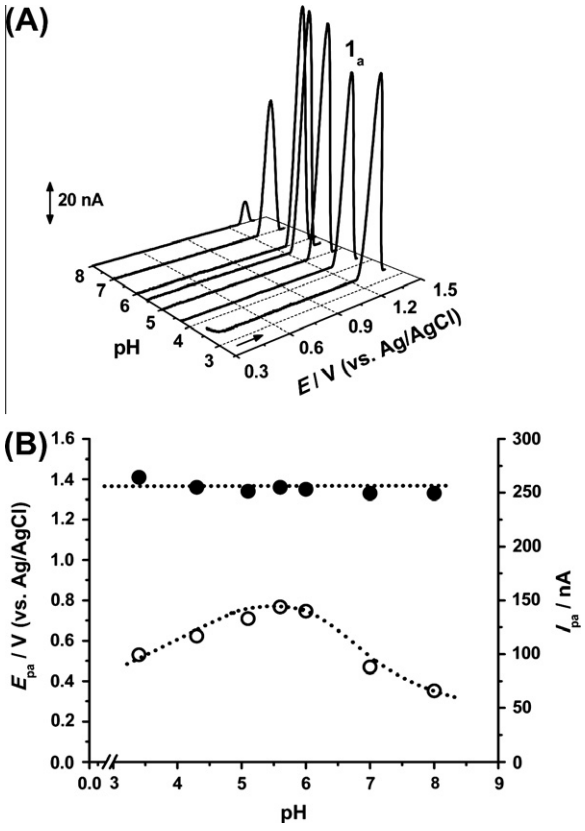

Fig. 3. (A) 3D plot of first DP voltammograms base-line corrected in 100 μM phosphotyrosine function of the pH of the supporting electrolyte. B) (●) E_{pa} and (○) I_{pa} of peak 1_a vs. pH.

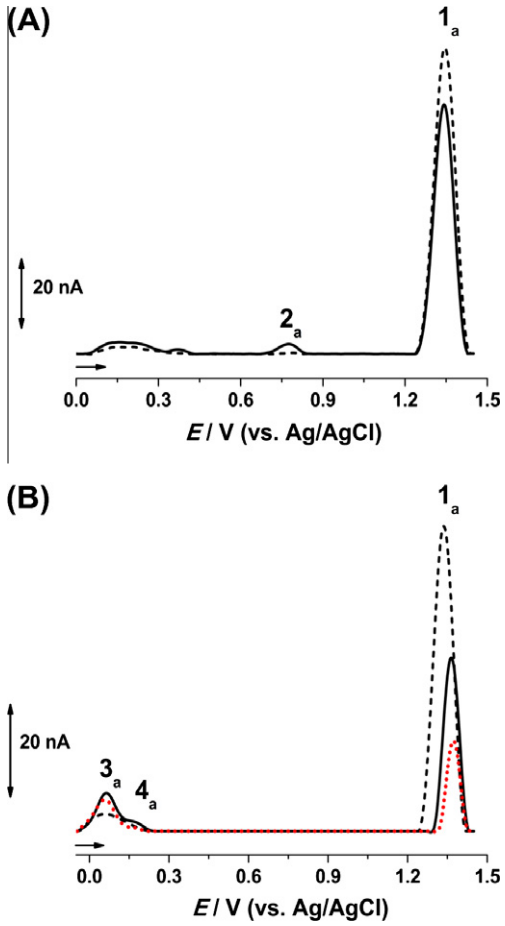

Fig. 4. DP voltammograms base-line corrected in 100 μM phosphotyrosine: (- - -) first and (––) second scans in pH: (A) 3.4 and (B) 7.0; (•••) first scan after transferring the electrode to the supporting electrolyte.

Peak 1_a current showed maximum values for 5.1 < pH < 6.1 while for other pH values the current got decreased. This effect is explained considering that the current registered upon application of a potential step in the case of an irreversible system is directly proportional with the rate constant of the heterogeneous electrochemical reaction [26,27]. Thus, the variation of peak 1_a current is due to the variation of the rate constant of the heterogeneous pTyr oxidation with the pH of the supporting electrolyte. On the other hand, a pH-dependent adsorption of pTyr and of its oxidation products at the GCE surface can influence the current of peak 1_a.

Consecutive DP voltammograms were recorded in 100 μM pTyr solutions in all supporting electrolytes. On the first DP voltammograms, peak 1_a appeared at E_{p1a} = +1.35 V.

On the second DP voltammogram in pH = 3.4, peak 2_a occurred at E_{p2a} = +0.77 V, Figs. 4A and S2A. Although two small shoulders were observed at lower potential values, their visualisation was difficult due to the functional groups such as the hydroxyls and carboxyls formed at the glassy carbon electrode surface [26].

In another experiment carried out in pH = 7.0, on the second voltammogram recorded in the solution of pTyr, two new peaks 3_a at E_{p3a} = +0.06 V and peak 4_a at E_{p4a} = +0.18 V appeared, Figs. 4B and S2B.

Peaks 2_a, 3_a and 4_a are due to pTyr oxidation products formed at the electrode surface after the first DP voltammogram.

The adsorption of the pTyr and its oxidation product at the GCE surface was confirmed when, at the end of several DP scans recorded in the solution containing pTyr, the electrode was washed with a jet of deionised water and then transferred to the supporting electrolyte. The DP voltammogram obtained in these conditions, Fig. 4B, showed the peaks 3_a and 4_a correspondent to pTyr oxidation products as well as peak 1_a due to the oxidation of pTyr adsorbed at the electrode surface.

In Fig. 5A, the second DP voltammograms recorded in solutions of 100 μM pTyr in different electrolytes were plotted. Peak 2_a occurred in electrolytes with pH < 5.6, and the peak current decreased with increasing pH, Fig. 5A. At the same time, both peaks 3_a and 4_a appeared on the second DP voltammograms and their currents increased with the pH, Fig. 5A.

Peaks 2_a, 3_a and 4_a were pH dependent, Fig. 5A and B. Their potentials occurred at lower positive values with increasing the pH. The relationships were linear, Fig. 5B, following the equations: E_{p2a} = 0.99–0.06 pH, E_{p3a} = 0.48–0.06 pH and E_{p4a} = 0.59–0.06 pH. The slopes of the lines, −60 mV per pH unit, have shown that the mechanisms of oxidation involved the same number of electrons and protons. The width at half-height of peak 2_a was $W_{1/2} \sim 90$ mV correspondent to the transfer of one electron. For both peaks 3_a and 4_a, $W_{1/2} \sim 50$ mV, close to the theoretical value for the transfer of two electrons [26].

3.2.2. Tyrosine

The electrochemical oxidation of tyrosine (Tyr) has been reviewed in order to obtain information about the pTyr oxidation mechanism.

DP voltammograms were recorded in solutions of 10 μM Tyr in different electrolytes with 0.1 M ionic strength, Fig. 6A. One main

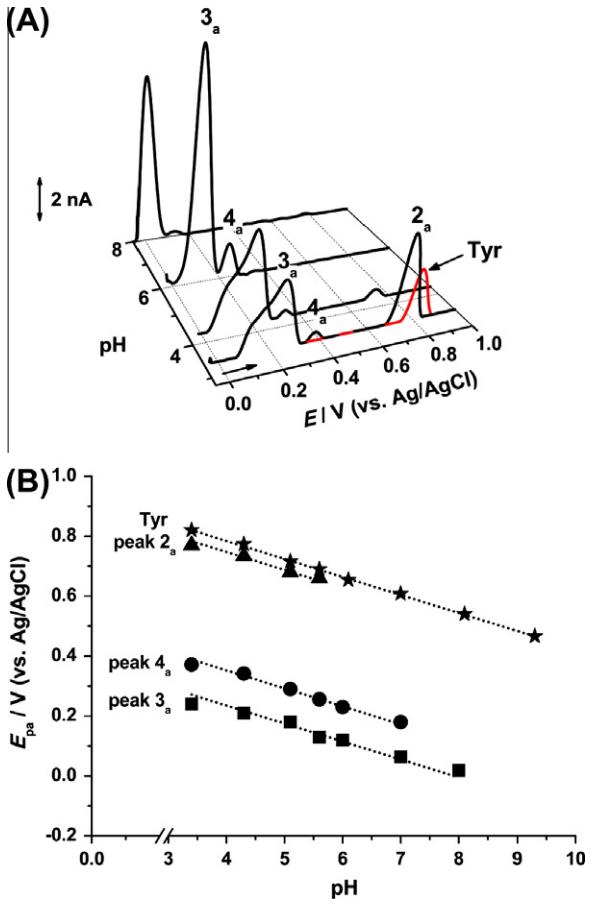

Fig. 5. (A) 3D plot of second DP voltammograms base-line corrected in 100 μM phosphotyrosine function of the pH of the supporting electrolyte and (—) DP voltammogram base-line corrected in 1 μM tyrosine in pH = 3.4. (B) Plot of E_{pa} of peaks 2_a, 3_a, 4_a of pTyr and peak of Tyr vs. pH of the supporting electrolyte.

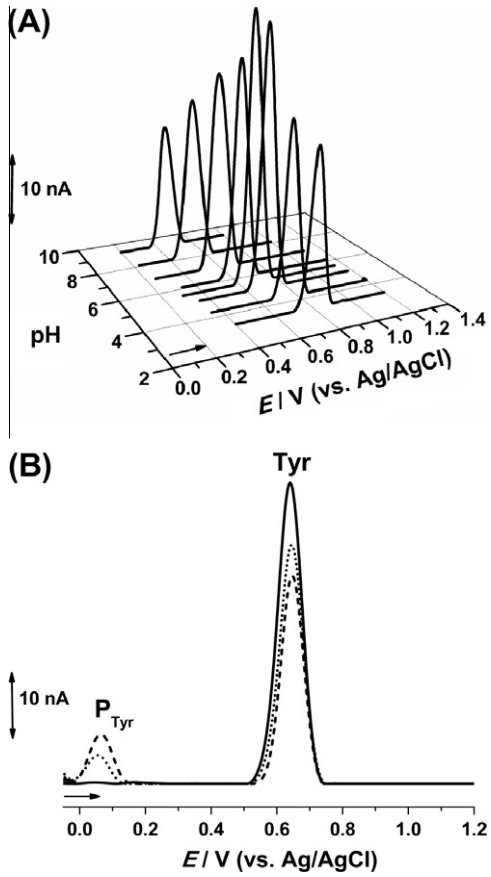

Fig. 6. DP voltammograms base-line corrected in 10 μM tyrosine: (A) function of the pH of the supporting electrolyte and (B) (––) first, (- - -) second and (···) third scans in pH = 7.0.

oxidation peak was observed and its potential turned less positive with increasing the pH of the supporting electrolyte. The dependence was linear following the equation E_{p2a} = 1.03–0.06 pH, Fig. 5B. The slope of the line was −60 mV per pH unit and the width at half-height of the Tyr oxidation peak $W_{1/2} \sim 90$ mV, correspondent to the transfer of one electron and one proton.

Consecutive DP voltammograms were recorded in 10 μM Tyr solutions in pH = 7.0, Fig. 6B. On the first DP voltammograms, the oxidation peak of Tyr occurred at E_{pa} = +0.61 V. On the second DP voltammogram, Fig. 6B, the peak at E_{pa} = +0.05 V was due to the oxidation product of Tyr formed at the GCE surface during the first scan. Similar experiments were carried out in all supporting electrolytes and only one oxidation product was observed.

The oxidation of Tyr involves the transfer of one electron and one proton from the hydroxyl group leading to a radical that reacts with water [28]. The only electroactive product formed is an *ortho*-quinone-like compound since the *para* position in Tyr moiety is occupied.

3.3. Square wave voltammetry

Since SWV allows lower detection limits than CV, this technique has been used in order to determine the character of the redox reactions of pTyr oxidation products. In SWV current is sampled in both positive and negative-going pulse, oxidation and reduction peaks of the electroactive compound at the electrode surface can be obtained simultaneously and the reversibility of the electron transfer reaction monitored by plotting the forward and backward components of the total current.

Successive SW voltammograms were recorded in a solution containing 200 μM pTyr in pH = 7.0, Fig. 7. On the first scan the anodic peak 1_a appeared at E_{p1a} = +1.37 V. The irreversibility of peak 1_a was confirmed by plotting the forward and backward components where only oxidation currents occurred, Fig. 7A.

By increasing the number of scans in solution, without cleaning the GCE surface, peaks 3_a and 4_a occurred at E_{p3a} = +0.15 V and at E_{p4a} = +0.28 V, Fig. 7B. The deconvolution of the total current recorded in these conditions has shown the reversibility of peaks 3_a and 4_a since by plotting the forward and backward components the reduction and oxidation currents were equal and occurred at the same potential value, Fig. 7B.

3.4. Oxidation mechanism

The electrochemical behaviour of phosphotyrosine was investigated using cyclic, differential pulse and square wave voltammetry. The CV study was very important as it enabled rapid screening of the electron transfer processes. SWV was more sensitive than CV and allowed the clarification of the reversibility of the electron transfer processes. DPV enabled the study of the coupled electron/proton transfer reactions, the formation of electroactive products, and their pH dependence.

Phosphotyrosine undergoes irreversible electrochemical oxidation, peak 1_a, Figs. 1, 2 and 7. The oxidation product of pTyr is electroactive, peak 2_a in Figs. 2B, 4A and 5A.

In order to obtain information about the origin of peak 2_a, experiments were carried out in Tyr solutions. It has been shown

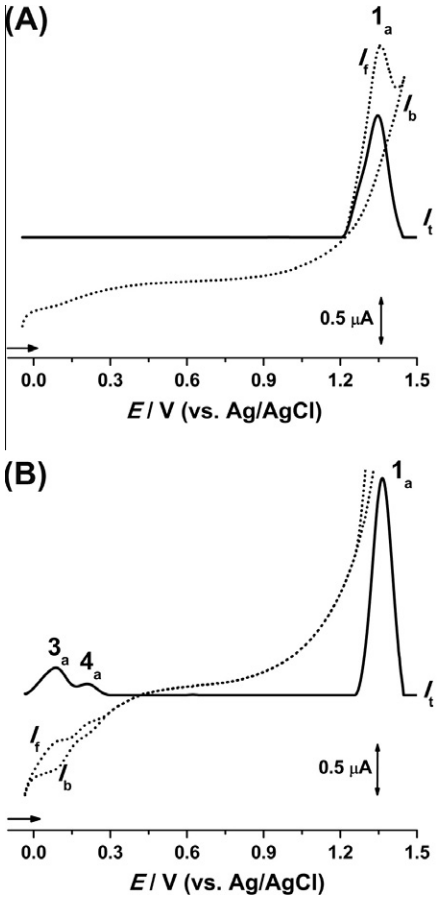

Fig. 7. SW voltammograms base-line corrected in 200 μM phosphotyrosine in pH = 7.0: (A) first and (B) third scan; I_t, I_f and I_b – total, forward and backward currents. Pulse amplitude 50 mV, f = 50 Hz and step potential 2 mV for a v = 100 mV s^{-1}.

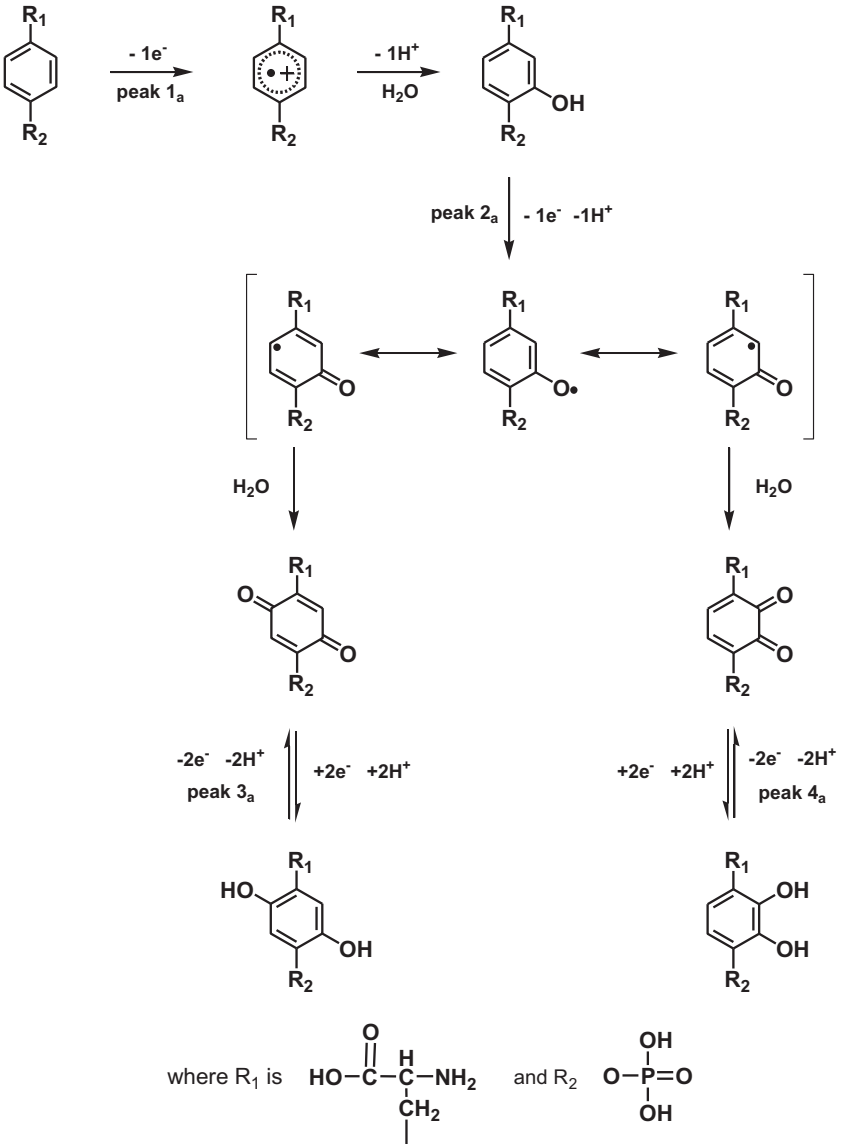

Scheme 2. Proposed oxidation mechanism of phosphotyrosine.

that the potential of peak 2_a is less positive than the oxidation of Tyr, Fig. 5A and B, thus excluding the possibility of Tyr formation during the electrochemical oxidation of pTyr.

Therefore, it is proposed that the oxidation mechanism of pTyr involves the transfer of one electron and no proton before the rate determining step, leading to the formation of a cation radical which undergoes chemical deprotonation and hydrolysis resulting in a phenol-like molecule, Scheme 2. Similar oxidation mechanisms were described for other substituted aromatic compounds [29,30].

The phenol-like pTyr redox product undergoes oxidation at peak 2_a with the transfer of one electron and one proton, Figs. 4 and 5 and Scheme 2, in agreement with the oxidation mechanism of phenol-substituted compounds [28]. This reaction involves the formation of a phenoxy radical stabilised by hydrolysis, Scheme 2, resulting *para*- and *ortho*-quinones species. These compounds undergo reversible redox reaction to hydroquinone and catechol, which are oxidised at peaks 3_a and 4_a, respectively, Scheme 2.

The oxidation of the pTyr redox products at peaks 2_a, 3_a and 4_a, occurs at lower values than the oxidation of pTyr, peak 1_a, Figs. 2B and 4A. For this reason, during the first voltammetric scan, pTyr and its redox products formed at the electrode surface are oxidised when reaching the maximum potential limit.

The irreversible oxidation of the phenol-like pTyr redox product at peak 2_a is more difficult in acid electrolytes [28]. In pH < 5.6 not all of pTyr redox product molecules are oxidised at the end of the first voltammetric scan. This allows the occurrence of peak 2_a on the second voltammograms in solutions with pH < 5.6, Figs. 2B, 4A and 5A.

By increasing the pH, the oxidation of the phenol-like pTyr redox product is facilitated. In these conditions, all molecules of the phenol-like pTyr redox product are oxidised when reaching the maximum potential limit during the first scan. Thus, peak 2_a does not occur on the second scan in solutions with pH > 5.6. Instead, the complete oxidation of the phenol-like pTyr redox product gives rise to the electroactive products that undergo oxidation at peaks 3_a and 4_a in Figs. 4B and 5A.

The two redox products correspondent to peaks 3_a and 4_a are the hydroquinone and catechol species that undergo reversible reactions, Fig. 7B, with the transfer of two electrons and two protons, Fig. 5 and Scheme 2, and the formation of *para*- and *ortho*-quinones.

4. Conclusion

The electrochemical investigation of phosphotyrosine redox behaviour was carried out using cyclic, differential pulse and square-wave voltammetry, in a wide pH range. It has been shown that phosphotyrosine undergoes oxidation at a glassy carbon electrode.

The electrochemical oxidation of phosphotyrosine is an irreversible process and occurs for electrolytes with pH < 9.0. The oxidation of phosphotyrosine is pH-independent and involves the transfer of one electron and no proton. For acid electrolytes one electroactive oxidation product that undergoes irreversible, one electron and one proton oxidation reaction was observed. For mild acid, neutral and alkaline electrolytes, two oxidation products undergo reversible, pH-dependent redox reactions with the transfer of two electrons and two protons. The electrochemical oxidation of tyrosine was also studied in order to find information about the redox products of phosphotyrosine. Based on the results obtained, a mechanism for oxidation of phosphotyrosine was proposed.

The study of the oxidation behaviour of phosphotyrosine is important for the determination of an analytical signal useful for the development of new methodologies for studying protein phosphorylation processes.

Acknowledgment

Financial support from Fundação para a Ciência e Tecnologia (FCT), Post-Doctoral Grant SFRH/BPD/36110/2007 (V.C. Diculescu), Project PTDC/SAU-BEB/104643/2008, POCI 2010 (co-financed by the European Community Fund FEDER), and CEMUC-R (Research Unit 285), is gratefully acknowledged.

Appendix A. Supplementary material

Supplementary data associated with this article can be found, in the online version, at http://dx.doi.org/10.1016/j.jelechem.2012.11.005.

References

[1] P. Patwardhan, W.T. Miller, Cell Signal. 19 (2007) 2218–2226.
[2] J.A. Ubersax, J.E. Ferrell Jr., Nat. Rev. Mol. Cell Biol. 8 (2007) 530–541.
[3] C.R. Hagan, A.R. Daniel, G.E. Dressing, C.A. Lange, Mol. Cell Endocrinol. 308 (2011) 133–138.
[4] Ahasanul Kobir, Lei Shi, Ana Boskovic, Christophe Grangeasse, Damjan Franjevic, Ivan Mijakovic, BBA-Gen Subjects 2011 (1810) 989–994.
[5] P. Blume-Jensen, T. Hunter, Nature 411 (2011) 355–365.
[6] S.F. Yan, E. Harja, M. Andrassy, T. Fujita, A.M. Schmidt, J. Am. Coll. Cardiol. 48 (2006) A47–A55.
[7] L.K. Chico, L.J. Van Eldik, D.M. Watterson, Nat. Rev. Drug Discov. 8 (2009) 892–909.
[8] A. Krupa, G. Preethi, N. Srinivasan, J. Mol. Biol. 339 (2004) 1025–1039.
[9] C. López-Otín, T. Hunter, Nat. Rev. Cancer 10 (2010) 278–293.
[10] M. Salvi, A.M. Brunati, A. Toninello, Free Radical. Biol. Med. 38 (2005) 1267–1277.
[11] D.W. Fry, Pharmacol. Therapeut. 82 (1999) 207–218.
[12] A. Levitzki, Cytokine Growth Fact. Rev. 15 (2004) 229–235.
[13] R. Roskoski Jr., Biochem. Biophys. Res. Commun. 324 (2004) 1155–1164.
[14] S. Wessler, S. Backert, Int. Rev. Cell Mol. Biol. 286 (2011) 271–300.
[15] M. Li, P. Luraghi, A. Amour, X.D. Qian, P.S. Carter, C.J. Clark, A. Deakin, J. Denyer, C.I. Hobbs, M. Surby, V.K. Patel, E.M. Schaefer, Anal. Biochem. 384 (2009) 56–67.
[16] Z. Yue, F. Zhuang, R. Kumar, I. Wong, S.B. Cronin, Y.H. Liu, Spectrochim. Acta A. Mol. Biomol. Spectrosc. 73 (2009) 226–230.
[17] I. Lázaro, M. Gonzalez, G. Roy, L.M. Villar, P. Gonzalez-Porqué, Anal. Biochem. 192 (1991) 257–261.
[18] J.A. Cooper, B.M. Sefton, T. Hunter, Methods Enzymol. 99 (1983) 387–402.
[19] J.Y.J. Wang, Anal. Biochem. 172 (1988) 1–7.
[20] A.M. Oliveira-Brett, A.M. Chiorcea Paquim, V.C. Diculescu, J.A.P. Piedade, Med. Eng. Phys. 28 (2006) 963–970.
[21] I.A. Rebelo, J.A.P. Piedade, A.M. Oliveira-Brett, Talanta 63 (2004) 323–331.
[22] K. Kerman, H.B. Kraatz, Biosens. Bioelectron. 24 (2009) 1484–1489.
[23] Y. Yang, L.H. Guo, N. Qu, M.Y. Wei, L.X. Zhao, B. Wan, Biosens. Bioelectron. 28 (2011) 284–290.
[24] K. Kerman, M. Vestergaard, M. Chikae, S. Yamamura, E. Tamiya, Electrochem. Commun. 9 (2007) 976–980.
[25] M. Chiku, K. Horisawa, N. Doi, H. Yanagawa, Y. Einaga, Biosens. Bioelectron. 26 (2010) 235–240.
[26] C.M.A. Brett, A.M. Oliveira Brett, Electrochemistry: Principles Methods and Applications, Oxford Science University Publications, Oxford, UK, 1993.
[27] A.J. Bard, L.R. Faulkner, Basic Potential Step Methods, in: Electrochemical Methods. Fundamentals and Applications, second ed., John Wiley & Sons, Inc., USA, 2001. (Chapter 5)
[28] T.A. Enache, A.M. Oliveira-Brett, J. Electroanal. Chem. 655 (2011) 9–16.
[29] D. Bejan, A. Savall, J. Electroanal. Chem. 507 (2001) 234–243.
[30] L.V. Costea, V.N. Bercean, V. Badea, G. Fafilek, A. Chiriac, Rev. Chim.-Bucharest 59 (2008) 691–693.